Phospholamban remains associated with the Ca^{2+}- and Mg^{2+}-dependent ATPase following phosphorylation by cAMP-dependent protein kinase

Sewite NEGASH, Qing YAO, Hongye SUN, Jinhui LI, Diana J. BIGELOW and Thomas C. SQUIER[1]

Biochemistry and Biophysics Section, Department of Molecular Biosciences, University of Kansas, Lawrence, KS 66045-2106, U.S.A.

We have used fluorescence and spin-label EPR spectroscopy to investigate how the phosphorylation of phospholamban (PLB) by cAMP-dependent protein kinase (PKA) modifies structural interactions between PLB and the Ca^{2+}- and Mg^{2+}-dependent ATPase (Ca-ATPase) that result in enzyme activation. Following covalent modification of *N*-terminal residues of PLB with dansyl chloride or the spin label 4-isothiocyanato-2,2,6,6-tetramethylpiperidine-*N*-oxyl ('ITC-TEMPO'), we have co-reconstituted PLB with affinity-purified Ca-ATPase isolated from skeletal sarcoplasmic reticulum (SR) with full retention of catalytic function. The Ca^{2+}-dependence of the ATPase activity of this reconstituted preparation is virtually identical with that observed using native cardiac SR before and after PLB phosphorylation, indicating that co-reconstituted sarcoplasmic/endoplasmic-reticulum Ca^{2+}-ATPase 1 (SERCA1) and PLB provide an equivalent experimental model for SERCA2a–PLB interactions. Phosphorylation of PLB in the absence of the Ca-ATPase results in a greater amplitude of rotational mobility, suggesting that the structural linkage between the transmembrane region and the N-terminus is destabilized. However, whereas co-reconstitution with the Ca-ATPase restricts the amplitude of rotational motion of PLB, subsequent phosphorylation of PLB does not significantly alter its rotational dynamics. Thus structural interactions between PLB and the Ca-ATPase that restrict the rotational mobility of the N-terminus of PLB are retained following the phosphorylation of PLB by PKA. On the other hand, the fluorescence intensity decay of bound dansyl is sensitive to the phosphorylation state of PLB, indicating that there are changes in the tertiary structure of PLB coincident with enzyme activation. These results suggest that PLB phosphorylation alters its structural interactions with the Ca-ATPase by inducing structural rearrangements between PLB and the Ca-ATPase within a defined complex that modulates Ca^{2+}-transport function.

Key words: Ca^{2+} transport, fluorescence spectroscopy, membrane reconstitution, protein–protein interactions, spin-label EPR.

INTRODUCTION

At submicromolar Ca^{2+} concentrations, the Ca^{2+}-transport activity of the Ca^{2+}- and Mg^{2+}-dependent ATPase (Ca-ATPase) in cardiac sarcoplasmic-reticulum (SR) membranes is regulated by phospholamban (PLB), a major target of the β-adrenergic cascade in the heart [1,2]. In the dephosphorylated state, PLB inhibits the Ca-ATPase. Phosphorylation of PLB at Ser^{16} or Thr^{17} by cAMP- or Ca^{2+}-calmodulin-dependent protein kinase respectively relieves this inhibition, resulting in more rapid rates of Ca^{2+} re-sequestration into the SR and thereby increasing the rate of cardiac relaxation [3–5]. The inhibitory effect of PLB on the Ca-ATPase has been suggested to involve the reversible binding of PLB to the Ca-ATPase, based largely on the observation that PLB modified with a photoactivatable cross-linker at Lys^{3} can be cross-linked to the Ca-ATPase before, but not after, phosphorylation of Ser^{16} of PLB [5,6]. Moreover, specific amino acid residues within the cytoplasmic domains of both PLB and the Ca-ATPase have been shown to be crucial for the functional inhibition of the Ca-ATPase by PLB [7,8]. Consistent with a specific binding interaction between PLB and the Ca-ATPase, recent measurements using proton NMR have demonstrated complex-formation between the Ca-ATPase and a peptide corresponding to the cytosolic domain of PLB [9]. Contact interactions between the N-terminal eight residues of PLB and the Ca-ATPase are retained following phosphorylation, suggesting that current models that emphasize the phosphorylation-dependent dissociation of PLB from the Ca-ATPase may not be correct [9,10]. However, a quantitative interpretation of these latter experiments is hampered by the inability of the peptide corresponding to the cytosolic domain of PLB to functionally regulate the Ca-ATPase under the conditions used in these experiments. Therefore, to identify possible alterations in the interactions between PLB and the Ca-ATPase that are affected by the phosphorylation of PLB, we have used spin-label EPR and fluorescence spectroscopy to measure the structural interaction between intact PLB and the Ca-ATPase in reconstituted membranes. In these reconstituted preparations the Ca-ATPase is fully regulated by the phosphorylation state of PLB. We find that PLB phosphorylation by cAMP-dependent protein kinase (PKA) results in small alterations in the tertiary structure, but that PLB remains motionally restricted by the Ca-ATPase. These results suggest that there are phosphorylation-dependent structural rearrangements between PLB and the Ca-ATPase within a stable oligomeric complex that modulate transport function.

A preliminary account of this work was presented at a symposium entitled 'Cardiac Sarcoplasmic Reticulum Function and Regulation of Contractility' sponsored by the New York Academy of Sciences [11].

Abbreviations used are: BAPTA, 1,2-bis-(*o*-aminophenoxy)ethane-*N,N,N′,N′*-tetra-acetic acid; Ca-ATPase, Ca^{2+}- and Mg^{2+}-dependent ATPase; $C_{12}E_9$, nona(ethylene glycol) dodecyl ether; CCCP, carbonyl cyanide 3-chlorophenylhydrazone; FD, frequency domain; ITC-TEMPO, 4-isothiocyanato-2,2,6,6-tetramethylpiperidine-*N*-oxyl; PKA, cAMP-dependent protein kinase; PLB, phospholamban; SR, sarcoplasmic reticulum; τ, mean fluorescence lifetime; ϕ, rotational correlation time; SERCA, sarcoplasmic/endoplasmic-reticulum Ca^{2+}-ATPase; L37A etc., $Leu^{37} \rightarrow$ Ala etc.

[1] To whom correspondence should be addressed (e-mail tsquier@ukans.edu).

EXPERIMENTAL

Materials

$CaCl_2$ standard solutions were purchased from VWR (St. Louis, MO, U.S.A.). Mops, KCl and ultracentrifugation-grade sucrose were purchased from Fisher (Fair Lawn, NJ, U.S.A.). Reactive Red 120 and the detergent *N*-octyl β-D-glucopyranoside were obtained from ICN (Aurora, OH, U.S.A.). Sepharose CL-4B, the detergent nona(ethylene glycol) dodecyl ether ($C_{12}E_9$), ADP, PKA, cAMP, ATP, $MgCl_2$, the Ca^{2+} ionophore A23187, the potassium ionophore valinomycin, EGTA and 4-isothiocyanato-2,2,6,6-tetramethylpiperidine-*N*-oxyl (ITC-TEMPO) were purchased from Sigma (St. Louis, MO, U.S.A.). The protonophore carbonyl cyanide 3-chlorophenylhydrazone (CCCP) was purchased from Fluka (Buchs, Switzerland). Dansyl chloride and the Ca^{2+}-sensitive dye 1,2-bis-(*o*-aminophenoxy)ethane-*N*,*N*,*N*′,*N*′-tetra-acetic acid (BAPTA) were purchased from Molecular Probes (Eugene, OR, U.S.A.). PLB was cloned into a pGEX-2T plasmid expression vector, expressed in JM109 *Escherichia coli* cells, and purified by preparative SDS/PAGE, as previously described [12]. Mouse monoclonal antibodies against this recombinant PLB were prepared and purified from ascites fluid using standard protocols [13]. SR vesicles were isolated from either rabbit skeletal fast-twitch muscle or porcine hearts as described previously [14,15]. Lipids were extracted from skeletal SR vesicles with organic solvents as previously described [16,17]. Ca-ATPase from skeletal SR was affinity-purified essentially as previously described [18,19]. Native and reconstituted vesicles containing the Ca-ATPase were stored at −70 °C.

Co-reconstitution of the Ca-ATPase with PLB

Unless otherwise specified, the purified Ca-ATPase was reconstituted in the presence of a 3-fold molar excess of PLB into lipids extracted from SR membranes, with minor modifications to established protocols [20,21]. Before reconstitution, 1.0 mg of extracted SR lipids was dried under nitrogen gas and kept in a vacuum desiccator overnight. The dried SR lipids were dispersed in approx. 0.5 ml of a reconstitution buffer [20 mM Mops (pH 7.0)/0.1 M KCl/0.1 mM $CaCl_2$/0.3 M sucrose] and solubilized by the addition of 12 mg of octyl glucoside. Separately, 200 μg of purified Ca-ATPase (≈2 nmol) was mixed with 36 μg of PLB (≈ 6 nmol), solubilized in 4 mg/ml $C_{12}E_9$ (or an equivalent volume of 4 mg/ml $C_{12}E_9$ when the Ca-ATPase was reconstituted without PLB) in a final volume of 100 μl. This mixture was then combined with the solubilized SR lipids, resulting in a final volume of 1.0 ml. To remove detergent, 100 mg of Bio-Beads SM-2™ (Bio-Rad, Richmond, CA, U.S.A.) was added, and the solution was incubated with gentle stirring for 1 h. Two more 100 mg aliquots of Bio-Beads were added at 1 h intervals. The resulting reconstituted vesicles were removed from the Bio-Beads and concentrated by centrifugation at 300000 g_{max} for 15 min. In order to minimize light-scattering for fluorescence measurements, the amount of lipid was decreased to equal the total mass of reconstituted protein. To enhance the fraction of PLB interacting with the Ca-ATPase, the amount of PLB included in the reconstitution was reduced to approx. 3 μg (≈ 0.5 nmol of PLB) for the majority of the spectroscopic measurements.

Enzymic and protein assays

The ATP-hydrolytic activity of the Ca-ATPase was determined by measuring the release of P_i [22], using either 10 or 100 μg of protein/ml in a solution containing 50 mM Mops (pH 7.0), 0.1 M KCl, 5 mM $MgCl_2$, 1 mM EGTA, 2 μM A23187, 1 μM CCCP, 2 μM valinomycin, 0.3 M sucrose and sufficient Ca^{2+} to yield the desired concentration of free Ca^{2+}. To phosphorylate PLB for enzyme-activity measurements, 10 μg of PKA/ml and 1 μM cAMP were also included in the assay buffer, incubating the solution at 25 °C for 10 min prior to the addition of 5 mM ATP to start the reaction. The extent of PLB phosphorylation induced by PKA involved incubation of proteoliposomes for 10 min in the presence of [γ-^{32}P]ATP (4500 c.p.m./nmol) in the presence of 0.5 μM free Ca^{2+}. The reaction was stopped by filtration on a glass filter, followed by washing with non-radioactive reaction buffer. Radioactivity associated with each filter was measured by liquid-scintillation counting. Non-specific radioactivity measured in the absence of PKA was subtracted from the total radioactivity. Protein concentrations of PLB stocks were determined by amino acid analysis. All other protein concentrations were determined by the Amido Black method [23].

Determination of Ca^{2+} binding affinities

To analyse the relative affinities and co-operative interactions between high-affinity Ca^{2+} binding sites on the Ca-ATPase, the Ca^{2+}-dependent activation of the Ca-ATPase was fit to the following equation:

$$\text{ATPase activity} = \frac{K_1[Ca^{2+}]_{free} + 2K_2[Ca^{2+}]^2_{free}}{2(1 + K_1[Ca^{2+}]_{free} + K_2[Ca^{2+}]^2_{free})} \quad (1)$$

ATPase activity represents the measured Ca^{2+}-dependent ATPase activity and is assumed to result from the fraction of Ca-ATPase polypeptide chains in which both high-affinity Ca^{2+} sites are occupied by Ca^{2+}. K_1 corresponds to the sum of the intrinsic equilibrium constants associated with Ca^{2+} binding to the two high-affinity binding sites on the Ca-ATPase (k_1 and k_2). K_2 represents the product of the intrinsic equilibrium constants k_1, k_2, and k_c, and explicitly takes into consideration co-operative interactions (k_c) between the high-affinity Ca^{2+}-binding sites [24].

Measurement of free Ca^{2+} concentrations

Free Ca^{2+} concentrations were determined using the Ca^{2+}-sensitive fluorophore BAPTA ($\lambda_{excitation} = 299$ nm; $\lambda_{emission} = 360$ nm), as previously described [25]. The dissociation constant (K_d) for Ca^{2+} binding to 4 μM BAPTA was measured to be 203 ± 7 nM in a buffer containing 20 mM Mops (pH 7.0), 0.1 M KCl, 5 mM $MgCl_2$, 5 mM ATP, 1 mM EGTA and various amounts of $CaCl_2$.

Covalent attachment of spectroscopic probes to PLB

Recombinant PLB reconstituted into lipid vesicles was incubated with a 5-fold molar excess of the spin label ITC-TEMPO in 20 mM Mops (pH 8.5)/0.1 M KCl at 25 °C in the dark for 5 h. Subsequently, the sample was centrifuged at 100000 g_{max} for 30 min. The resulting pellet was resuspended in 20 mM Mops (pH 7.0)/0.3 M sucrose. The stoichiometry of ITC-TEMPO labelling was determined from a comparison of the integrated intensities of the labelled sample with known standards, essentially as previously described [26]. Alternatively, for fluorescence experiments, 200 μg of PLB in 4 mg/ml $C_{12}E_9$ and 20 mM Mops, pH 8.0, were incubated with a 20-fold molar excess of dansyl chloride for 5 h in the dark at room temperature. The reaction was stopped by addition of 10-fold excess lysine, incubating for an additional 45 min in order to allow it to bind with unreacted probe. After exhaustive dialysis against 2 mg/ml

$C_{12}E_9$/20 mM Mops, pH 7.0, the stoichiometry of labelling was determined from the molar absorption coefficient (ϵ_{344} 4600 $M^{-1} \cdot cm^{-1}$ [27]). Protein concentration was determined by the Amido Black method [23].

Spin-label EPR spectroscopy

EPR spectra were measured using a Bruker (Acton, MA, U.S.A.) ESP-300E spectrometer, using 100 kHz field modulation with a peak-to-peak amplitude (H_m) of 2.0 and a microwave field amplitude (H_1) of about 10 μT (0.1 G). Oxygen was removed from samples using gas-permeable TPX sample cells (Medical Advances, Milwaukee, WI, U.S.A.) purged with nitrogen gas. Temperature was controlled using a Bruker model B-VT 2000 Eurotherm temperature controller. Spectra were taken at 4 °C at a protein concentration of 10 mg/ml. Phosphoylatation of PLB for EPR experiments was carried out essentially as previously described [15,28].

Analysis of spin-label EPR spectra

In the slow motional regime, the effective rotational correlation time (in seconds) can be estimated from the separation between the low- and high-field extrema (i.e. $T'_{\parallel}$) in comparison with these values in the rigid limit (i.e. $T^{r}_{\parallel}$), where there is no detectable rotational motion, where:

$$\tau_r = 5.4 \times 10^{-10}\left[1-\left(\frac{T'_{\parallel}}{T^{r}_{\parallel}}\right)^{-1.36}\right] \quad (2)$$

The value of $T^{r}_{\parallel}$ was determined to be 3.4 mT (34.3 G) for ITC-TEMPO, essentially as previously described [29]. These measurements involved cross-linking a mutant calmodulin spin-labelled with ITC-TEMPO at a single cysteine engineered at position 69 to isothiocyanato-glass beads.

Fluorescence measurements

All steady-state fluorescence measurements were measured using a Spex Industries (Edison, NJ, U.S.A.) FluoroMax-2 spectrofluorimeter. Frequency-domain lifetime and anisotropy measurements were measured using an ISS (Champaign, IL, U.S.A.) K2 fluorimeter, essentially as previously described [30]. Excitation involved the 333 nm output from a Coherent (Santa Clara, CA, U.S.A.) Innova 400 argon ion laser, and the emitted light was collected subsequent to a GG400 long-pass filter. Fluorescence measurements of reconstituted samples (50 μg/ml) were made at 25 °C in 50 mM Mops (pH 7.0)/0.1 M KCl/1 mM EGTA/5 mM $MgCl_2$/5 mM ATP/0.6 mM $CaCl_2$, resulting in $[Ca^{2+}]_{free}$ = 0.5 μM. To phosphorylate PLB, 40 μg/m1 PKA and 1 μM cAMP were also included in the assay medium.

Analysis of fluorescence intensity decays

The time-dependent intensity decay $I(t)$ of dansyl bound to PLB was fitted by using the method of non-linear least squares to a sum of exponentials, essentially as previously described [30,31], where:

$$I(t) = \sum_{i=1}^{n} \alpha_i \, e^{-t/\tau_i} \quad (3)$$

α_i are the normalized pre-exponential factors, τ_i are the excited state decay times, and n is the number of exponential components required to describe the decay. The parameter values are determined by minimizing the χ_R^2 (the F statistic), which serves as a goodness-of-fit parameter that provides a quantitative comparison of the adequacy of different assumed models [32]. Subsequent to the measurement of the intensity decay, the mean lifetime, $\bar{\tau}$, was calculated:

$$\bar{\tau} = \sum_{i=1}^{n} \alpha_i \tau_i \quad (4)$$

where the amplitude weighing implies a direct relationship between $\bar{\tau}$ and the quantum yield of the fluorophore [33].

Analysis of fluorescence anisotropy decays

The differential-phase and modulated-anisotropy parameters describing the anisotropy decay were fit to a multiexponential model using mathematical transforms that have been previously described in detail [30,34]:

$$r(t) = (r_0 - r_\infty) \times \sum_{i=1}^{n} g_i \, e^{\frac{-t}{\phi_i}} + r_\infty \quad (5)$$

where r_0 is the limiting anisotropy in the absence of rotational diffusion, ϕ_i are the rotational correlation times, $r_0 \times g_i$ are the amplitudes of the total anisotropy loss associated with each rotational correlation time, r_∞ is the residual anisotropy, and n is the total number of components associated with the exponential decay. The goodness-of-fit was determined through a comparison of the deviations between the measured and calculated values. Errors in the differential phase and modulated anisotropy were assumed to be 0.2 and 0.005 respectively.

RESULTS

Functional co-reconstitution of the Ca-ATPase

PLB expressed and purified from *E. coli* was co-reconstituted with affinity-purified Ca-ATPase at a molar ratio of three PLBs per Ca-ATPase using lipids extracted from SR membranes, essentially as previously described [20,21]. The fast-twitch skeletal-muscle sarcoplasmic/endoplasmic-reticulum Ca^{2+}-ATPase (SERCA1) was used in these experiments on the basis of (i) its greater stability in detergent compared with that of SERCA2a expressed in cardiac SR and (ii) previous demonstrations that SERCA1 is fully regulated by PLB and can functionally substitute for SERCA2a in the heart [19,35–37]. In agreement with previous results, we find a similar activation of the Ca-ATPase for reconstituted and native cardiac preparations upon phosphorylation of PLB by PKA or increasing Ca^{2+} concentration (Figure 1). Moreover, values of the maximal catalytic activity (i.e. V_{max}) for reconstituted vesicles are in good agreement with those for native SR membranes when differences in Ca-ATPase enrichment are taken into account. Thus the inhibitory interactions between PLB and the SERCA1 isoform of the Ca-ATPase in these reconstituted preparations are both qualitatively and quantitatively similar to those of SERCA2a in native cardiac SR membranes. Addition of the Ca^{2+} ionophore A23187 to either reconstituted vesicles or native cardiac SR results in the same 2-fold stimulation of ATPase activity, indicating that reconstituted vesicles are tightly sealed. Detergent solubilization of reconstituted vesicles with $C_{12}E_9$ results in no further stimulation of activity compared with that induced by A23187. Thus detergent solubilization only alters Ca^{2+} permeability and does not make additional catalytic sites of the Ca-ATPase available to substrates. These results indicate an asymmetrical reconstitution of the Ca-ATPase. In contrast, PLB is symmetrically reconstituted, as assessed by the ability to release approximately one-half of the cytosolic domain labelled with the fluorophore dansyl chloride. Thus, following exhaustive trypsin digestion, 44 ± 9 %

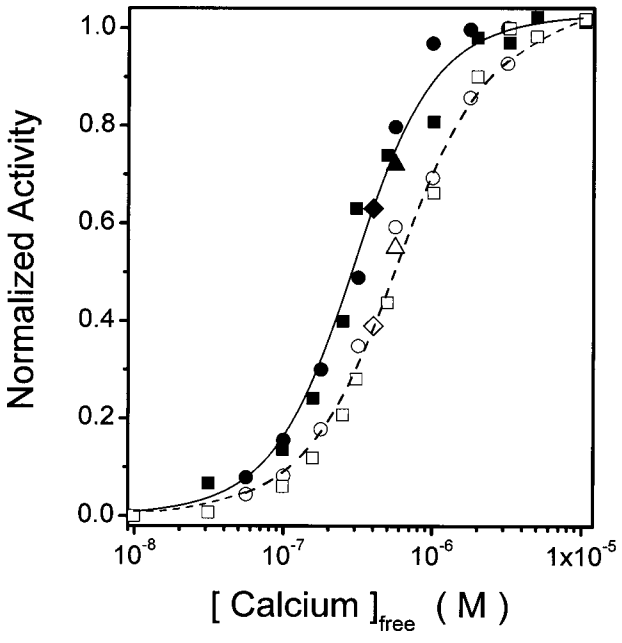

Figure 1 Ca^{2+}-dependence of ATPase activity

Rates of ATP hydrolysis of the Ca-ATPase in native cardiac SR membranes (□,■) or of the Ca-ATPase co-reconstituted with native PLB (○,●) or subsequent to the covalent attachment of dansyl chloride (△,▲) or ITC-TEMPO (◇,◆) in the absence (□,○,△,◇) or presence (■,●,▲,◆) of PKA. Data for native cardiac SR are taken from [15]. Experimental curves were obtained using eqn. (1) before (broken line) and after (continuous line) PLB phosphorylation, where the concentration of calcium necessary for half-maximal activation ($K_{\frac{1}{2}}^{1}$) is respectively 0.57 ± 0.06 μM and 0.29 ± 0.03 μM before and after the phosphorylation of PLB. Fitting the data to eqn. (1) yields the following macroscopic equilibrium constants K_1 and K_2, which before PLB phosphorylation are $(1.5 \pm 0.4) \times 10^6$ M^{-1} and $(3.0 \pm 0.4) \times 10^{12}$ M^{-1} and, following PLB phosphorylation, are $(1.9 \pm 0.7) \times 10^6$ M^{-1} and $(1.1 \pm 0.1) \times 10^{13}$ M^{-1}. Standard deviations of individual measurements are no more than 8% of the indicated values. Maximal Ca^{2+}-dependent ATPase activities were 4.0 ± 0.1 and 1.0 ± 0.1 μmol of $P_i \cdot mg^{-1} \cdot min^{-1}$ for the Ca-ATPase co-reconstituted with PLB and cardiac SR membranes respectively.

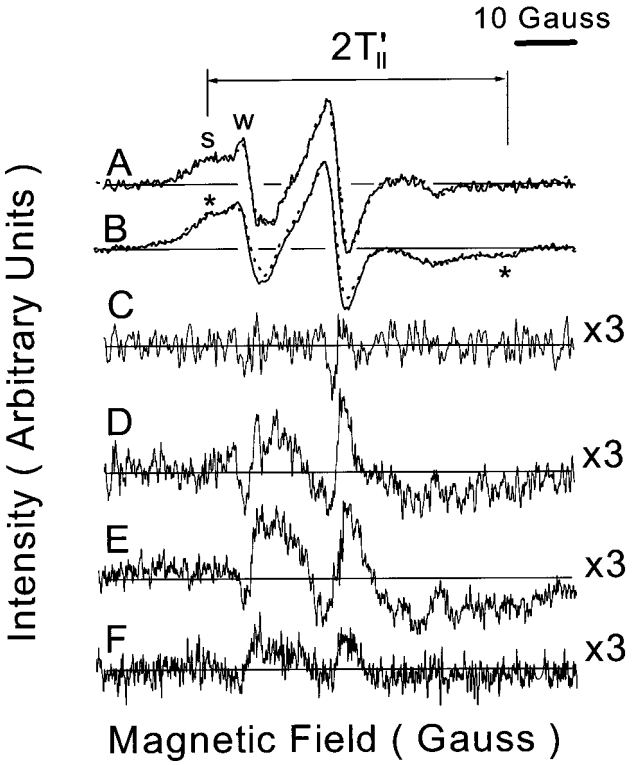

Figure 2 EPR spectra of spin-labelled PLB

PLB reconstituted in lipids extracted from SR membranes in the absence (trace **A**) or presence (trace **B**) of the Ca-ATPase, either before (continuous line) or after (dotted line) the phosphorylation of PLB by PKA. Strongly (S) and weakly (W) immobilized spin populations are apparent. In all cases, the strongly immobilized (S) spectral component has a maximal hyperfine splitting ($2T'_{||}$) of 5.28 ± 0.03 mT (52.8 ± 0.3 G) (*), indicating that spin-labelled PLB has an effective rotational correlation time of 3.6 ± 0.2 ns (see eqn 2 in the Experimental section). This latter result is in good agreement with the fluorescence-anisotropy data, whose average rotational correlation time (i.e. $\Sigma_j g_j \times \phi_j$) is 3.9 ns. Residuals (traces **C**–**F**) represent the result of the following spectral subtractions: PLB–P_i minus PLB (trace **C**), Ca-ATPase:PLB minus PLB (trace **D**), Ca-ATPase:PLB–P_i minus PLB–P_i (trace **E**) and Ca-ATPase:PLB–P_i minus Ca-ATPase:PLB (trace **F**). Spectra are normalized to the same concentration of spin labels.

of the cytosolic portions of PLB (covalently modified with dansyl chloride) was released into the supernatant following reconstitution in either the absence or presence of the Ca-ATPase. Consistent with this result, the stoichiometry of PLB phosphorylation by PKA was measured to be 0.38 ± 0.08 mol of phosphate/mol of PLB. Thus essentially all available sites on PLB are phosphorylated by PKA. These results, coupled with the fact that the extent of regulation following co-reconstitution of PLB with the Ca-ATPase is equivalent to native cardiac SR vesicles, indicate that there is a preferential association between Ca-ATPase with PLB molecules whose cytosolic domain faces the vesicle exterior.

Covalent modification of PLB with spectroscopic probes

To detect changes in the physical interaction between PLB and the Ca-ATPase, we have purified and covalently modified PLB using either ITC-TEMPO or dansyl-chloride prior to reconstitution with the Ca-ATPase (see the Experimental section). Both spectroscopic probes are known to react with primary amines under these labelling conditions [27]. Therefore the spectroscopic labels are expected to modify the two free amino groups in expressed PLB located at the N-terminus and at Lys^3. Consistent with this expectation, we find that, on average, 1.3 ± 0.2 and 1.9 ± 0.2 mol of ITC-TEMPO or dansyl chloride respectively are bound to each mol of PLB. PLB retains its ability to regulate fully the Ca-ATPase after it has been derivatized with either probe, and activation of ATPase activity at submicromolar Ca^{2+} concentrations is similar to that observed for unmodified PLB (Figure 1). Thus neither spectroscopic probe interferes with specific functional interactions between PLB and the Ca-ATPase or with the phosphorylation of PLB by PKA, permitting their use in investigating physiologically relevant interactions between PLB and the Ca-ATPase.

Spin-label EPR measurements of PLB rotational dynamics

We have used EPR spectroscopy to investigate interactions between spin-labelled PLB and the Ca-ATPase, and to detect possible changes in these interactions as a result of the phosphorylation of PLB by PKA (Figure 2). In order to maximize the sensitivity to structural interactions between PLB and the Ca-ATPase, these measurements were made using reconstituted proteoliposomes with amounts of PLB substoichiometric to the Ca-ATPase. These experimental conditions minimize any fraction of PLB molecules not associated with the Ca-ATPase. A comparison between the rotational dynamics of PLB reconstituted into SR lipids alone relative to those observed following

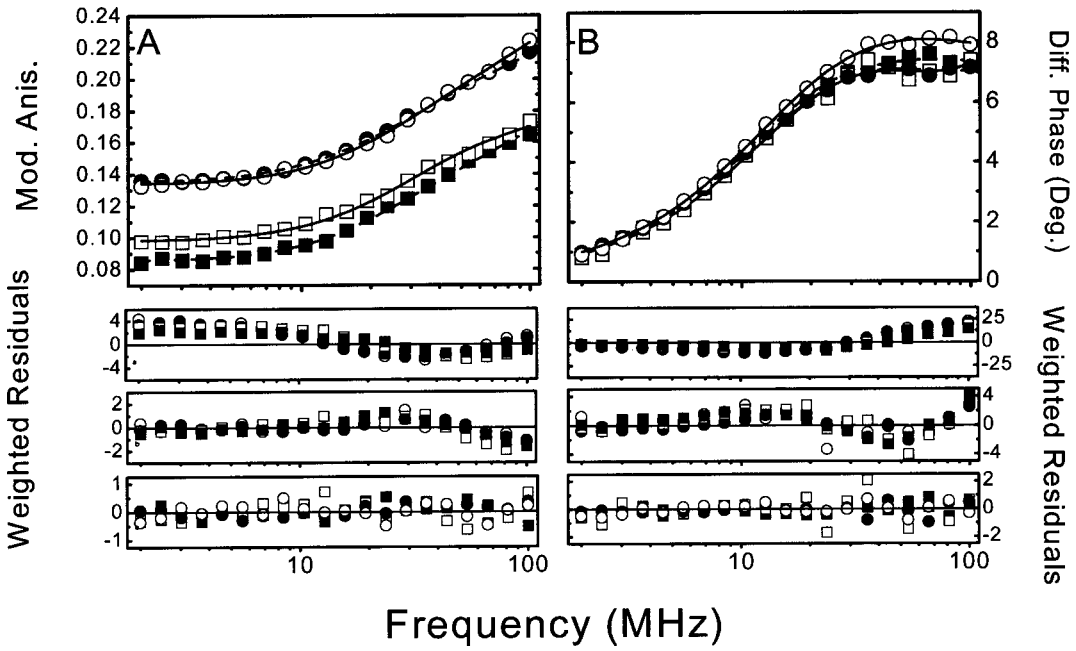

Figure 3 Rotational dynamics of dansyl-PLB

Frequency-domain-anisotropy data and the respective least-squared fits to the data are shown for PLB reconstituted in the absence (□,■) or presence (○,●) of the Ca-ATPase either before (□,○; continuous line) or after (■,●; broken line) phosphorylation by PKA for both the modulated anisotropy (Mod. Anis.) (**A**) and differential phase (**B**). The weighted residuals are shown below each plot for models of increasing complexity, corresponding to one, two and three component fits to the data using eqn. (5) in the Experimental section, and represent the difference between the experimental and calculated values normalized by the assumed errors for the modulated anisotropy (0.005) and differential phase (0.2°). Sample conditions were as described in the legend to Table 1.

co-reconstitution with the Ca-ATPase reveals significant spectral differences, as indicated by the large non-zero residuals following spectral subtraction (Figure 2, traces D and E). The spectral lineshape of PLB reconstituted only in the presence of SR lipids is characterized by (i) a weakly immobilized component ('w'), indicative of fast nanosecond rotational motion, and (ii) a broad strongly immobilized component ('s'), representing a less mobile population of spins (Figure 2, trace A). This latter result is consistent with the covalent attachment of the ITC-TEMPO chromophore to two distinct sites on PLB (see above). After co-reconstitution of PLB with the Ca-ATPase, the weakly immobiled spin-population (w) exhibited a reduced peak-height (L_{pp}) and increased linewidth (Γ_m), indicating a reduced rotational mobility (Figure 2, trace B). On the other hand, neither the maximal hyperfine splitting of the immobilized component (i.e. $2T'_{\parallel}$) nor the relative area ($L_{pp} \times \Gamma_m^2$) of the mobile component is significantly altered by the presence of the Ca-ATPase. Thus no substantial changes in the polarity surrounding the ITC-TEMPO spin label or in the fractional contribution of these two spectral components are observed upon co-reconstitution with the Ca-ATPase. These results indicate that the Ca-ATPase functions to decrease the rotational motion of PLB, consistent with previous suggestions of a direct physical interaction between PLB and the Ca-ATPase [6,9,28,38]. Phosphorylation of PLB with PKA results in little or no change in the spectral lineshape relative to that observed for the non-phosphorylated sample, irrespective of the presence of the Ca-ATPase (Figure 2, traces C and F). These results indicate that the phosphorylation of PLB does not significantly alter its rotational dynamics on the spin-label EPR timescale. Since phosphorylation has little effect on the structural interaction between PLB and the Ca-ATPase, these results suggest that phosphorylated PLB remains associated with the Ca-ATPase.

Fluorescence anisotropy measurements of PLB rotational dynamics

Frequency-domain measurements of the fluorescence anisotropy decay of dansyl-labelled PLB have been used as a complementary measurement of the rotational dynamics of PLB to assess the structural interaction between PLB and the Ca-ATPase (Figure 3). It should be noted that the large Stokes shift of the dansyl-chromophore precludes homotransfer between chromophores in close proximity, since the absorption of the dansyl-chromophore does not significantly overlap the fluorescence emission spectrum (results not shown). Thus it is possible to obtain an unambiguous measurement of the rotational dynamics of the PLB [39,40]. To measure the dynamic structure of PLB, we collected data over 20 frequencies between 2.0 and 100 MHz (Figure 3). On increasing the frequency, the differential phase and modulated anisotropy progressively increase. Substantial differences are observed for dansyl-PLB reconstituted in the absence or presence of the Ca-ATPase, which are particularly apparent in the frequency-dependent response for the modulated anisotropy (Figure 3A). These results are consistent with spin-label EPR measurements, which also detect the structural interaction between PLB and the Ca-ATPase (see above).

To assess the physical reasons for observed differences in the anisotropy decays resulting from reconstitution of PLB in the presence of the Ca-ATPase, we have fitted the data to a sum of exponentials using previously described algorithms [30,34]. In all cases the fluorescence anisotropy decays of dansyl-PLB were adequately fitted to a model consisting of two rotational correlation times plus a residual anisotropy (r_∞), as indicated by the randomly weighted residuals (Figure 3; Table 1). Inclusion of additional fitting parameters results in no significant improvement in the calculated fit to the data. It should be noted that

Table 1 Rotational dynamics of dansyl-PLB reconstituted in the presence and absence of the Ca-ATPase

Average values are shown for the pre-exponential amplitude factors ($g_i \times r_0$), rotational correlation times (ϕ_i) and residual anisotropies (r_∞) obtained from multi-exponential fits for two or three independent data sets, using eqn. (5) in the Experimental section. The initial anisotropy, r_0, is 0.26 ± 0.01. S.E.M. values are shown in parentheses. Measurements involved 50 μg/ml reconstituted sample in the absence ('Control') or presence of 40 μg/ml PKA and 1 μM cAMP ('+PKA') in 50 mM Mops (pH 7.0)/0.1 M KCl/5 mM $MgCl_2$/5 mM ATP/1 mM EGTA, and sufficient $CaCl_2$ to result in 0.5 μM free calcium.

Sample	Conditions	$g_1 \times r_0$	ϕ_1 (ns)	$g_2 \times r_0$	ϕ_2 (ns)	r_∞
PLB	Control	0.121 (0.001)	0.8 (0.2)	0.096 (0.003)	7.8 (0.4)	0.043 (0.003)
	+PKA	0.116 (0.003)	1.2 (0.1)	0.112 (0.003)*	9.0 (0.6)	0.029 (0.002)*
PLB + Ca-ATPase (5-fold molar excess PLB)	Control	0.116 (0.001)	1.3 (0.1)	0.102 (0.004)	7.9 (0.2)	0.066 (0.002)
	+PKA	0.114 (0.001)	1.2 (0.3)	0.111 (0.009)	8.1 (0.7)	0.060 (0.001)
PLB + Ca-ATPase (1.5-fold molar excess PLB)	Control	0.096 (0.001)	1.2 (0.1)	0.086 (0.005)	7.7 (0.3)	0.076 (0.001)
	+PKA	0.093 (0.002)	1.1 (0.3)	0.087 (0.008)	8.3 (0.3)	0.080 (0.001)

* Statistical differences relative to the corresponding control samples computed using Student's *t*-test, where $P < 0.05$ [69]; the temperature was 25 °C.

the residual anisotropies associated with PLB reconstituted in the presence and absence of the Ca-ATPase are proportional to the modulated anisotropy apparent at low frequencies (Figure 3A). In these measurements, the rotational correlation times (ϕ_i) are a measure of both the hydrodynamic volume and direct structural interactions involving the backbone fold of PLB in the vicinity of the dansyl-chromophore with the Ca-ATPase. In contrast, the amplitude terms ($g_i \times r_0$) or the residual anisotropy (r_∞) are indicative of long-range structural linkages between the N-terminal domain and the bilayer, which may be affected by binding interactions with the Ca-ATPase.

The large residual anisotropy associated with dansyl-labelled PLB indicates that the rotational dynamics of the N-terminal domain of PLB is highly restricted, irrespective of the presence of the Ca-ATPase. This latter result is consistent with earlier suggestions that PLB contains an ordered secondary structure between the N-terminus and transmembrane domains [41,43]. On co-reconstitution of the Ca-ATPase with a fivefold molar excess of PLB, one observes a small increase in the rotational correlation time (ϕ_1) and a small decrease in the amplitude of motion ($g_1 \times r_0$) associated with the sub-nanosecond rotational motion of the backbone fold near the N-terminus of PLB (Table 1). A larger increase in the residual anisotropy (r_∞) is observed. These results indicate that the Ca-ATPase functions to restrict the rotational dynamics of PLB. Under these conditions there is an excess of PLB relative to the Ca-ATPase, and it is expected that a substantial proportion of PLB does not associate directly with the Ca-ATPase. Decreasing the amount of PLB relative to the Ca-ATPase (i.e. 1.5-fold molar excess of PLB) results in a further decrease in the rotational mobility, suggesting that a larger proportion of PLB is undergoing a direct interaction with the Ca-ATPase. Under these latter conditions there are now substantial decreases in the amplitude terms (i.e. g_1 and g_2) associated with both segmental motion of the dansyl chromophore (ϕ_1) and the slower overall rotational motion of PLB (ϕ_2). There is an associated increase in the residual anisotropy (r_∞), which is substantially larger than that observed when a 5-fold molar excess of PLB is co-reconstituted with the Ca-ATPase. In comparison with the computed parameters obtained in the presence of 5-fold excess PLB relative to the Ca-ATPase, we observe that the change in the pre-exponential amplitude term ($g_1 \times r_0$) associated with the segmental motion of the dansyl-chromophore is approximately 5-fold larger. A comparison of the change in $g_2 \times r_0$ is complicated by the fact that this parameter is essentially unchanged in the presence of a 5-fold excess of PLB relative to the Ca-ATPase. Thus, under experimental conditions where a larger fraction of PLB interacts with the Ca-ATPase, there is a further reduction in the rotational mobility of PLB, indicating that interaction with the Ca-ATPase functions to alter the dynamic structure of PLB. It should be noted that, since both monomers and pentamers of PLB have been suggested to interact directly with the Ca-ATPase [44], and the distribution of oligomeric forms of PLB in association with the Ca-ATPase cannot be estimated from the current data, observed changes in rotational mobility do not precisely correlate with the molar ratio of PLB relative to the Ca-ATPase.

Effects of PLB phosphorylation on the dynamic structure of PLB

The substantial differences in the anisotropy decay of PLB reconstituted in the absence and presence of the Ca-ATPase provides a convenient means to detect possible changes in the structural interactions between PLB and the Ca-ATPase that result from the phosphorylation by PKA. Using low PLB stoichiometries, where interactions between PLB and the Ca-ATPase are enhanced, we observe that the phosphorylation of PLB results in no significant changes in the frequency response of the modulated anisotropy or differential phase of PLB co-reconstituted with the Ca-ATPase (Figure 3; Table 1). Thus PLB remains motionally restricted by the Ca-ATPase after its phosphorylation by PKA. In contrast, upon phosphorylation of PLB in the absence of the Ca-ATPase, there is a small reduction in the residual anisotropy, as evidenced by the smaller modulated anisotropy observed at low frequencies (Figure 3A). This result is consistent with earlier proposals suggesting that the phosphorylation of PLB disrupts the secondary structure of PLB [41,42], resulting in increased conformational disorder and rotational mobility. Interaction with the Ca-ATPase prevents these phosphorylation-dependent conformational changes and alters the structural coupling between the transmembrane and cytosolic portions of PLB.

Fluorescence lifetime measurements

The excited state lifetime of the bound dansyl group provides information regarding the structure and environment of the N-terminal region of PLB. Therefore we have measured the frequency response of the phase shift and modulation of intensity-modulated light at 20 frequencies between 2.0 and 100 MHz for the dansyl-chromophore covalently bound to PLB reconstituted in the absence and presence of the Ca-ATPase. In all cases, the

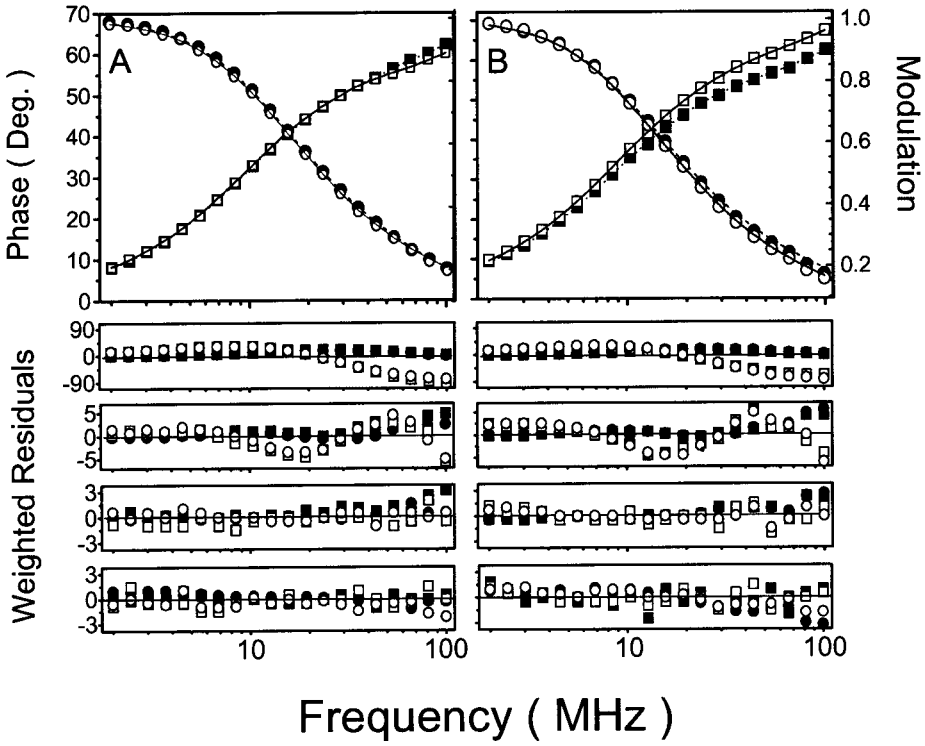

Figure 4 Fluorescence lifetime data for dansyl-PLB

The frequency response of the phase shift (□,■) and modulation (○,●) for PLB reconstituted in the absence (**A**) or presence (**B**) of the Ca-ATPase either before (□,○) or after (■,●) phosphorylation by PKA. Lines represent the best fit to the data before (continuous line) and after (dotted line) PLB phosphorylation, as described in the Experimental section. Below each data set are the weighted residuals, corresponding to models of increasing complexity involving one, two, three and four exponential fits to the data using eqn. (3) in the Experimental section. The weighted residuals correspond to the difference between the experimental data and the experimental fit normalized by the experimental error associated with the phase (0.2 °) and modulation (0.005). Sample conditions were as described in the legend to Table 2.

Table 2 Lifetime data for dansyl-PLB reconstituted in the presence or absence of Ca-ATPase

Shown are average values for the amplitudes (α_i) and lifetimes (τ_i) obtained from multi-exponential fits for three independent data sets, using eqn. (3) in the Experimental section. S.E.M. values are shown in parentheses. Measurements were made at 25 °C using 50 μg/ml reconstituted sample in the absence ('Control') or presence of 40 μg/ml PKA and 1 μM cAMP ('+PKA') in 50 mM Mops (pH 7.0)/0.1 M KCl/5 mM $MgCl_2$/5 mM ATP/1 mM EGTA, and sufficient $CaCl_2$ to result in 0.5 μM free calcium. Samples were reconstituted with 1.5 mol of PLB/mol of Ca-ATPase.

Sample	Conditions	α_1	τ_1 (ns)	α_2	τ_2 (ns)	α_3	τ_3 (ns)	$\bar{\tau}$ (ns)*
PLB	Control	0.59 (0.01)	1.1 (0.1)	0.17 (0.01)	6.0 (0.5)	0.24 (0.01)	14.9 (0.4)	5.3 (0.1)
	+PKA	0.42 (0.09)	0.9 (0.3)	0.25 (0.04)	3.4 (0.8)	0.33 (0.05)	14.0 (0.2)	5.8 (0.4)
PLB + Ca-ATPase	Control	0.44 (0.02)	1.2 (0.2)	0.21 (0.02)	5.7 (0.8)	0.35 (0.01)	16.0 (0.3)	7.4 (0.2)
	+PKA	0.56 (0.02)†	1.3 (0.1)	0.20 (0.02)	7.0 (0.5)	0.24 (0.03)†	17.2 (0.7)	6.2 (0.1)†

* $\tau = \Sigma\ \alpha_i\ \tau_i$, which is directly related to the quantum yield [33].

† Statistical differences relative to the corresponding control samples computed using Student's *t*-test, where $P < 0.05$ [69].

intensity decays of dansyl-PLB are adequately described by a three-exponential fit, as indicated by the randomly weighted residuals (Figure 4). We observe that there are substantial differences in the amplitude-weighting factors associated with the fluorescence-intensity decays of dansyl-PLB reconstituted in the absence and presence of the Ca-ATPase (Table 2). As a result the mean fluorescence lifetime of dansyl-PLB increases from 5.3 ± 0.1 ns to 7.4 ± 0.2 ns. Under these latter conditions the emission maximum of dansyl-PLB ($\lambda_{max} = 496$ nm) remains essentially unchanged. These results are consistent with spin-label EPR data, where the unchanged maximal hyperfine splitting ($2T'_{\parallel}$) also indicates that PLB phosphorylation does not result in large alterations in the polarity near the N-terminus of PLB (Figure 2). These differences in the fluorescence-intensity decays of PLB reconstituted in the absence and presence of the Ca-ATPase suggests that there are substantial differences in tertiary structures of PLB upon association with the Ca-ATPase [45]. The greater sensitivity of excited-state lifetime measurements to the structural interactions between PLB and the Ca-ATPase relative to spectral shifts thus permits the detection of possible changes in the tertiary structure of PLB that occurs as a result of the phosphorylation of PLB (see below).

Influence of PLB phosphorylation on fluorescence intensity decays

The sensitivity of the intensity decay of dansyl-PLB to interactions with the Ca-ATPase permits an assessment of possible changes in the interactions between PLB and the Ca-ATPase associated with enzyme activation following phosphorylation by PKA. When PLB is reconstituted alone in SR lipids, phosphorylation-dependent shifts in the frequency response are not observed (Figure 4A; Table 2). On fitting the data one observes that the parameters describing the intensity decay of dansyl-PLB are essentially unchanged. Thus phosphorylation at Ser^{16} does not significantly alter the polarity in the vicinity of the dansyl moiety bound near the N-terminus. In contrast, when PLB is co-reconstituted with the Ca-ATPase, there is a reproducible shift in the frequency response of dansyl-PLB toward higher frequencies (Figure 4B), indicating a shorter mean fluorescence lifetime ($\bar{\tau}$). Upon fitting the data for the intensity decay of PLB co-reconstituted in the presence of the Ca-ATPase one finds that there are substantial changes in the amplitude terms associated with the intensity decay following the phosphorylation of PLB by PKA (Table 2). These results indicate that there are structural changes in the vicinity of the N-terminus that may reflect either changes in the secondary structure of PLB or direct binding interactions with the Ca-ATPase. These results suggest a structural coupling between the phosphorylation of Ser^{16} and the environment near the N-terminal region of PLB that is dependent upon interaction with the Ca-ATPase.

DISCUSSION

Summary of results

We have used spin-label EPR and fluorescence spectroscopy to measure dynamic structural interactions between PLB and the SERCA1 isoform of the Ca-ATPase in a functionally reconstituted preparation. Irrespective of the presence of the Ca-ATPase, the N-terminal domain of PLB is motionally restricted. These results indicate a structural coupling between the transmembrane and N-terminal portions of PLB (Figures 2 and 3). However, the presence of the Ca-ATPase further restricts the amplitude of rotational motion, resulting in a significant increase both in the linewidth of the weakly immobilized component (w), in the EPR spectra of spin-labelled PLB (Figure 2) and in the residual anisotropy (r_∞) of dansyl-PLB (Figure 3; Table 1). There are no corresponding changes in the rates of rotational motion (i.e. ϕ_1 or ϕ_2), indicating that neither the N-terminus nor the probe sites themselves are directly involved in contact interactions with the Ca-ATPase. Therefore observed alterations in the fluorescence lifetime intensity decay and the associated restriction in the rotational motional of dansyl-PLB in the presence of the Ca-ATPase result from tertiary structural changes near the N-terminus of PLB induced by long-range contact interactions between sites on PLB with the Ca-ATPase (Figure 4; Table 2). Phosphorylation-induced changes in the fluorescence intensity decay of dansyl-PLB occur only following co-reconstitution with the Ca-ATPase, indicating that there are changes in the structural coupling between the cytosolic domain of PLB and the Ca-ATPase that correlate with the modulation of Ca-ATPase function (Table 2). Thus these results provide direct evidence that the activation of the Ca-ATPase resulting from the phosphorylation of PLB is due to the modulation of the structural coupling between the cytosolic domain of PLB and the Ca-ATPase. However, since PLB remains motionally restricted by the Ca-ATPase following phosphorylation, these results indicate that regulation of Ca-ATPase function involves modulation of the structural coupling between a stable oligomeric complex involving PLB and the Ca-ATPase.

Mechanisms of PLB inhibition of Ca-ATPase function

It has been known for some time that PLB is a major target of the β-adrenergic cascade in the heart [4,46–48]. Phosphorylation of PLB results in a shift in the Ca^{2+}-dependence of the catalytic activity of the Ca-ATPase (Figure 1), resulting in activation of the Ca-ATPase at submicromolar free-Ca^{2+} concentrations with little or no alteration in the maximal velocity of the Ca-ATPase [36,49,50]. The similarity between the Ca^{2+}-dependence of Ca-ATPase transport activity found in activated cardiac SR (after phosphorylation of PLB) and that of the Ca-ATPase found in skeletal muscle SR (in which PLB is not expressed) suggests that dephosphorylated PLB acts as an inhibitor of the Ca-ATPase [46]. The mechanisms underlying the inhibitory action of PLB on Ca-ATPase function have been the subject of much interest. Direct measurements of Ca^{2+} binding and detailed kinetic measurements indicate that PLB does not alter the Ca^{2+} affinity of the Ca-ATPase, but rather suggests an altered activation barrier associated with the slow isomerization step of Ca^{2+} activation [15,51]. The nature of the structural coupling between PLB and the Ca-ATPase has been investigated through the addition to cardiac SR vesicles of monoclonal antibodies raised against PLB. Addition of these antibodies stimulates Ca-ATPase activity under non-saturating Ca^{2+} concentrations in a manner identical with that associated with the direct activation of PLB through covalent phosphorylation [51,52]. These latter results suggested that activation of the Ca-ATPase involves the disruption of structural interactions between PLB and the Ca-ATPase. Consistent with this latter hypothesis, the extent of chemical cross-linking between the Ca-ATPase and a peptide identical with the cytoplasmic domain of PLB is decreased upon the phosphorylation of PLB [6,9,44,53,54]. The ability of polyanions (e.g. heparin) to activate the Ca-ATPase suggests that it is the increased negative charge associated with phosphorylation that modulates the interactions between PLB and the Ca-ATPase [55].

Using site-directed mutagenesis and after co-expression of PLB mutants with the Ca-ATPase, the structural interactions between PLB and the Ca-ATPase were subsequently demonstrated to involve direct contact interactions between both the cytoplasmic and transmembrane domains of PLB and the Ca-ATPase [8,56]. The porcine cardiac SERCA2a isoform of the Ca-ATPase contains a sequence, i.e. $KDDKPVK^{402}$, that is required for the functional interaction between PLB and the Ca-ATPase [6,36,50], suggesting that these residues may comprise a critical binding region. The homologous SERCA1 isoform of rabbit skeletal muscle has a similar sequence, $KNDKPIR^{402}$, and when co-reconstituted with PLB is similarly regulated by changes in the phosphorylation of PLB. Specific binding site(s) within transmembrane helix M6 within the nucleotide-binding domain of the SERCA1 isoform of the Ca-ATPase have been identified that interact with PLB transmembrane sequences, and co-expression of the transmembrane sequence, alone, of PLB with the Ca-ATPase has been shown to inhibit transport activity at submicromolar Ca^{2+} concentrations [56,57]. However, while the relative roles of the cytosolic and transmembrane portions of PLB in the functional regulation of the Ca-ATPase remain unclear, it has been suggested that they function in concert through a long-range structural linkage involving conformational coupling through the Ca-ATPase [7,8,59]. Consistent with this latter suggestion, the interaction between PLB and the Ca-ATPase has been shown to modulate

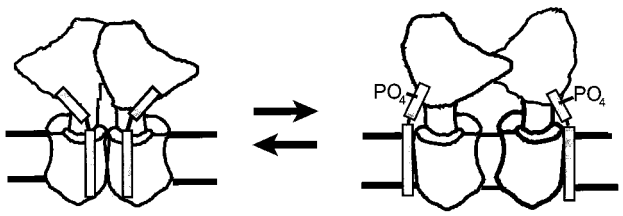

Scheme 1 Model depicting possible interactions between PLB and the Ca-ATPase

PLB is shown as a monomeric unit interacting with each Ca-ATPase; two Ca-ATPase·PLB heterodimers interact as a functional unit. Activation of the Ca-ATPase by PKA is suggested to require the phosphorylation of two PLB molecules within a dimeric complex containing two Ca-ATPase polypeptide chains. Phosphorylation of both PLB molecules results in conformational changes both to PLB and to the Ca-ATPase, including the spatial rearrangement of Ca-ATPase polypeptide chains with respect to one another, as previously shown to be associated with enzyme activation by PKA [15,38,60]. Conformational changes of PLB, largely undefined as yet, exclude its dissociation from the Ca-ATPase. Larger oligomers of PLB (not shown) are not directly involved in the functional regulation of the Ca-ATPase. The overall shape of the Ca-ATPase is highly asymmetrical, and was derived from the 1.4 nm (14 Å) resolution image obtained using image-enhanced cryo-electron microscopy [70,71]. The approximate location of PLB relative to the tertiary structure of the Ca-ATPase is consistent with the location of sequences within the cytosolic (i.e. $KNDKPIR^{402}$) and transmembrane (i.e. helix M6) portions of the Ca-ATPase that interact with PLB [72].

dynamic structural changes normally associated with the Ca^{2+} transport mechanism [15,28,38,60]. However, these previous measurements provided no direct evidence with respect to the nature of the structural coupling between PLB and the Ca-ATPase responsible for enzyme activation. We have now shown, in the present study, that the structural coupling between the cytosolic portion of PLB and the Ca-ATPase responsible for enzyme activation does not involve the dissociation of PLB from the Ca-ATPase, as previously proposed [6,8,10]. Rather, the structural coupling between the cytosolic portions of PLB and the Ca-ATPase is retained following the phosphorylation of PLB. The physical nature of this regulatory mechanism therefore involves tertiary structural changes within PLB that result from phosphorylation, which alter the sites of interaction between cytosolic portions of PLB and the Ca-ATPase.

Oligomeric state of PLB

PLB is a highly hydrophobic 52-amino-acid protein, which self-associates in detergents [58]. Native PLB exhibits a preference for monomeric and pentameric associations on SDS/PAGE; a similar distribution of oligomeric species has been observed when reconstituted into lipid membranes [62]. Site-directed mutagenesis of specific amino acids in the primary sequence of PLB [e.g. L37A ($Leu^{37} \rightarrow Ala$), C41F] has been shown to disrupt the formation of oligomeric species on SDS/PAGE without compromising the ability of these mutant PLB species to regulate Ca-ATPase transport activity in membranes [8,36,61,59]. Likewise the average oligomeric state of PLB is smaller in the presence of the Ca-ATPase [63]. As a result, it has been suggested that monomeric and pentameric forms of PLB exist in equilibrium within biological membranes, with the monomeric form of PLB acting as the physiological inhibitor of the Ca-ATPase, while pentamers represent a self-aggregated free pool of PLB [59,62]. Since phosphorylation stabilizes oligomeric forms of PLB reconstituted in the absence of the Ca-ATPase [62], it has been suggested that the regulation of the Ca-ATPase by PLB involves phosphorylation-dependent changes in the dynamic equilibrium between oligomeric and monomeric states of PLB [5,8,10,63]. However, no prior measurements have directly measured changes in the structural interaction between PLB and the Ca-ATPase in functionally active membrane preparations. The present results, which indicate a retention in the structural interaction between PLB and the Ca-ATPase, demonstrate that the regulation of the Ca-ATPase as a result of the phosphorylation of PLB is the result of changes in the structural interaction between PLB and the Ca-ATPase within a defined oligomeric complex (Scheme 1).

Phosphorylation-dependent changes in PLB structure

Available structural information regarding phosphorylation-dependent structural changes of PLB has been largely based on measurements either of peptides corresponding to the cytosolic domain of PLB, or of the entire PLB molecule, in the absence of the Ca-ATPase [5]. For example, evidence has been presented that the phosphorylation of PLB results in localized structural changes that modify the quantum yield of Tyr^6 that correlate with increases in the apparent Stokes radius of PLB in SDS [64,65]. Solid-state NMR and molecular-dynamics simulations suggest that the mechanisms underlying these phosphorylation-dependent structural changes primarily involve increases in the conformational flexibility between Thr^{17} and Pro^{22} [66,67]. Our observation that phosphorylation induces decreases in the substantial residual anisotropy of dansyl-PLB reconstituted in the absence of the Ca-ATPase is consistent with these suggestions (Figure 3; Table 1). The magnitude of the residual anisotropy measured from the fluorescence anisotropy decay of dansyl-labelled PLB is directly proportional to the extent of motional restriction. Therefore an approximation of the magnitude of this conformational change can be calculated by assuming a symmetrical rotational motion of the principle transition dipoles of dansyl to be along the major axis of PLB [68]. These calculations suggest that there is a 5 ± 1 ° change (i.e. from 58 ± 1 ° to 63 ± 1 °) in the orientation of PLB relative to the membrane normal upon phosphorylation of PLB. This structural change is not observed when the Ca-ATPase is present in functionally reconstituted membranes, indicating that interactions with the Ca-ATPase restrict the dynamic structure of the cytosolic domain of PLB.

Conclusions and future directions

Direct structural interactions between PLB and the Ca-ATPase occur within biological membranes, and these structural interactions are modulated by the phosphorylation of PLB at Ser^{16} by PKA. These interactions involve modest structural rearrangements between PLB and the Ca-ATPase within a defined oligomeric complex of Ca-ATPase and PLB. Future studies should focus on the identification of specific contact interactions between PLB and the Ca-ATPase using functionally reconstituted preparations, and how these interactions change as a result of the phosphorylation of PLB.

This work was supported by the National Institutes of Health (grants GM 46837 and AG 12275) and the American Heart Association (Kansas Affiliate). We thank Professor Suren Tatulian for insightful discussions and Swee Yong Goh for technical assistance in the expression and purification of PLB.

REFERENCES

1 Kranias, E. G. and Solaro, R. J. (1982) Phosphorylation of troponin I and phospholamban during catecholamine stimulation of rabbit heart. Nature (London) **298**, 182–184

2 Stokes, D. L. (1997) Keeping Ca^{2+} in its place. Curr. Opin. Struct. Biol. **7**, 550–556.

3 Lindemann, J. P., Jones, L. R., Hathaway, D. R., Henry, B. G. and Watanabe, A. M. (1983) β-Adrenergic stimulation of phospholamban phosphorylation and Ca^{2+}-ATPase activity in guinea pig ventricles. J. Biol. Chem. **258**, 464–471

4 Simmerman, H. K., Collins, J. H., Theibert, J. L., Wegener, A. D. and Jones, L. R. (1986) Sequence analysis of phospholamban. Identification of phosphorylation sites and two major structural domains. J. Biol. Chem. **261**, 13333–13341

5 Simmerman, H. K. and Jones, L. R. (1998) Phospholamban: protein structure, mechanism of action and role in cardiac function. Physiol. Rev. **78**, 921–947

6 James, P., Inui, M., Tada, M., Chiesi, M. and Carafoli, E. (1989) Nature and site of phospholamban regulation of the Ca^{2+} pump of sarcoplasmic reticulum. Nature (London) **342**, 90–92.

7 MacLennan, D. H., Toyofuku, T. and Kimura, Y. (1997) Sites of regulatory interaction between Ca^{2+} ATPases and phospholamban. Basic Res. Cardiol. **92**, 11–15

8 MacLennan, D. H., Kimura, Y. and Toyofuku, T. (1998) Sites of regulatory interaction between Ca^{2+} ATPases and phospholamban. Ann. N. Y. Acad. Sci. **853**, 31–42

9 Levine, B. A., Patchell, V. B., Sharma, P., Gao, Y., Bigelow, D. J., Yao, Q., Goh, S., Colyer, J., Drago, G. A. and Perry, S. V. (1999) Sites on the cytoplasmic region of phospholamban involved in interaction with the Ca^{2+}-activated ATPase of the sarcoplasmic reticulum. Eur. J. Biochem. **264**, 905–913

10 Thomas, D. D., Reddy, L. G., Karim, C. B., Cornea, R., Autry, J. M., Jones, L. R. and Stamm, J. (1998) Direct spectroscopic detection of molecular dynamics and interactions of the Ca^{2+} pump and phospholamban. Ann. N.Y. Acad. Sci. **853**, 186–194

11 Negash, S., Sun, H., Yao, Q., Goh, S., Bigelow, D. and Squier, T. (1998) Cytosolic domain of phospholamban remains associated with the Ca-ATPase following phosphorylation by cAMP-dependent protein kinase. Ann. N.Y. Acad. Sci. **853**, 288–291

12 Yao, Q., Bevan, J. L., Weaver, R. F. and Bigelow, D. J. (1996) Purification of porcine phospholamban expressed in *Escherichia coli*. Protein Expression Purif. **8**, 463–468

13 Fambrough, D. M. and Bayne, E. K. (1983) Multiple forms of $(Na^+ + K^+)$-ATPase in the chicken. Selective detection of the major nerve, skeletal muscle and kidney form by a monoclonal antibody. J. Biol. Chem. **258**, 3926–3935

14 Fernandez, J. L., Rosemblatt, M. and Hidalgo, C. (1980) Highly purified sarcoplasmic reticulum vesicles are devoid of Ca^{2+}-independent ('basal') ATPase activity. Biochim. Biophys. Acta **599**, 552–568

15 Negash, S., Chen, L. T., Bigelow, D. J. and Squier, T. C. (1996) Phosphorylation of phospholamban by cAMP-dependent protein kinase enhances interactions between Ca-ATPase polypeptide chains in cardiac sarcoplasmic reticulum membranes. Biochemistry **35**, 11247–11259

16 Chen, P. S., Toribara, T. Y. and Warner, H (1956) Microdetermination of phosphorus. Anal. Chem. **28**, 1756–1758

17 Hidalgo, C., Ikemoto, N. and Gergely, J. (1976) Role of phospholipids in the Ca^{2+}-dependent ATPase of the sarcoplasmic reticulum. Enzymatic and ESR studies with phospholipid-replaced membranes. J. Biol. Chem. **251**, 4224–4232

18 Coll, R. J. and Murphy, A. J. (1984) Purification of the Ca-ATPase of sarcoplasmic reticulum by affinity chromatography. J Biol Chem. **259**, 14249–14254

19 Yao, Q., Chen, L. T. and Bigelow, D. J. (1998) Affinity purification of the Ca-ATPase from cardiac sarcoplasmic reticulum membranes. Protein Expression Purif. **13**, 191–197

20 Szymalska, G., Kim, H. W. and Kranias, E. G. (1991) Reconstitution of the skeletal sarcoplasmic reticulum Ca^{2+}-pump: Influence of negatively charged phospholipids. Biochim. Biophys. Acta **1091**, 127–134

21 Reddy, L. G., Jones, L. R., Cala, S. E., O'Brian, J. J., Tatulian, S. A. and Stokes, D. L. (1995) Functional reconstitution of recombinant phospholamban with rabbit skeletal Ca^{2+}-ATPase. J. Biol. Chem. **270**, 9390–9397

22 Lanzetta, P. A., Alvarez, L. J., Reinach, P. S. and Candia, O. A. (1979) An improved assay for nanomole amounts of inorganic phosphate. Anal. Biochem. **100**, 95–97

23 Schaffner, W. and Weissmann, C. (1973) A rapid sensitive and specific method for the determination of protein in dilute solution. Anal. Biochem. **56**, 502–514

24 Pedigo, S. and Shea, M. A. (1995) Discontinuous equilibrium titrations of cooperative Ca^{2+} binding to calmodulin monitored by 1-D ^{1}H-nuclear magnetic resonance spectroscopy. Biochemistry **34**, 10676–10689

25 Swenson, C. A. and Fredricksen, R. S. (1992) Interaction of troponin C and troponin C fragments with troponin I and troponin I inhibitory peptide. Biochemistry **31**, 3420–3429

26 Squier, T. C. and Thomas, D. D. (1989) Selective detection of the rotational dynamics of the immobilized lipid in sarcoplasmic reticulum membranes. Biophys. J. **56**, 735–748

27 Haugland, R. (1996) Handbook of Fluorescent Probes and Research Chemicals, Molecular Probes, Inc., Eugene, OR

28 Voss, J., Jones, L. R. and Thomas, D. D. (1994) The physical mechanism of Ca^{2+} pump regulation in the heart. Biophys. J. **67**, 190–196

29 Szczesna, D. and Fajer, P. J. (1995) The tropomyosin domain is flexible and disordered in reconstituted thin filaments. Biochemistry **34**, 3614–3620

30 Hunter, G. W. and Squier, T. C. (1998) Phospholipid acyl chain dynamics are independent of headgroup structure in binary mixtures of dioleoyl-phosphatidylcholine and dioleoyl-phosphatidylethanolamine. Biochim. Biophys. Acta **1415**, 63–76

31 Bevington, P. R. (1969) Data Reduction and Error Analysis for the Physical Sciences, McGraw Hill, Inc., New York

32 Lakowicz, J. R. and Gryczynski, I. (1991) Frequency-domain fluorescence spectroscopy. In Topics in Fluorescence Spectroscopy (Lakowicz, J. R., ed.), vol. 1, pp. 293–335, Plenum Press, New York

33 Luedtke, R., Owen, C. S., Vanderkooi, J. M. and Karush, F. (1981) Proximity relationships within the F_c segment of rabbit immunoglobulin G analyzed by resonance energy transfer. Biochemistry **20**, 2927–2936

34 Weber, G. (1981) Resolution of the fluorescence lifetimes in a heterogeneous system by phase and modulation measurements. J. Phys. Chem. **85**, 949–953

35 Toyofuku, T., Kurzydlowski, K., Tada, M. and MacLennan, D. H. (1993) Identification of regions in the Ca^{2+}-ATPase of sarcoplasmic reticulum that affect functional association with phospholamban. J. Biol. Chem. **268**, 2809–2815

36 Toyofuku, T., Kurzydlowski, K., Tada, M. and MacLennan, D. H. (1994) Amino acids Lys-Asp-Asp-Lys-Pro-Val^{402} in the Ca($^{2+}$)-ATPase of cardiac sarcoplasmic reticulum are critical for functional association with phospholamban. J. Biol. Chem. **269**, 22929–22932

37 Ji, Y., Loukianov, E., Loukianov, T., Jones, L. R. and Periasamy, M. (1999) SERCA1a can functionally substitute for SERCA2a in the heart. Am. J. Physiol. **276**, H89–H97

38 Negash, S., Huang, S. and Squier, T. C. (1999) Rearrangement of domain elements of the Ca-ATPase in cardiac sarcoplasmic reticulum membranes upon phospholamban phosphorylation. Biochemistry **38**, 8150–8158

39 Lakowicz, J. R. (1983) Principles of Fluorescence Spectroscopy, Plenum Press, New York

40 Blackman, S. M., Piston, D. W. and Beth, A. H. (1998) Oligomeric state of human erythrocyte band 3 measured by fluorescence resonance energy homotransfer. Biophys. J. **75**, 1117–1130

41 Tatulian, S. A., Jones, L. R., Reddy, L. G., Stokes, D. L. and Tamm, L. K. (1995) Secondary structure and orientation of phospholamban reconstituted in supported bilayers from polarized attenuated total reflection FTIR spectroscopy. Biochemistry **34**, 4448–4456

42 Mayer, E. J., McKenna, E., Garsky, V. M., Burke, C. J., Mach, H., Middaugh, C. R., Sardana, M., Smith, J. S. and Johnson, Jr., R. G. (1996) Biochemical and biophysical comparison of native and chemically phospholamban and a monomeric phospholamban analog. J. Biol. Chem. **271**, 1669–1677

43 Arkin, I. T., Rothman, M., Ludlam, C. F., Aimoto, S., Engelman, D. M., Rothschild, K. J. and Smith, S. O. (1995) Structural model of the phospholamban ion channel complex in phospholipid membranes. J. Mol. Biol. **248**, 824–834

44 Hunter, G. W., Karim, C. B., Sheen, C., Barany, G. and Thomas, D. D. (2000) Oligomeric structure does not influence the extent of interactions between phospholamban and the Ca-ATPase from sarcoplasmic reticulum. Biophys. J. **78**, 75a

45 Royer, C. A. (1993) Understanding fluorescence decays in proteins. Biophys. J. **65**, 9–10

46 Kranias, E. G. (1985) Regulation of Ca^{2+} transport by protein phosphatase activity associated with cardiac sarcoplasmic reticulum. J. Biol. Chem. **260**, 11006–11010

47 Tada, M., Kadoma, M., Inui, M. and Fujii, J. (1988) Regulation of Ca^{2+}-pump from cardiac sarcoplasmic reticulum. Methods Enzymol. **157**, 107–154

48 Jones, L. R., Wegener, A. D. and Simmerman, H. K. (1988) Purification of phospholamban from canine cardiac sarcoplasmic reticulum vesicles by use of sulfhydryl group affinity chromatography. Methods Enzymol. **157**, 360–369

49 Sasaki, T., Inui, M., Kimura, Y., Kuzuya, T. and Tada, M. (1992) Molecular mechanism of regulation of Ca^{2+} pump ATPase by phospholamban in cardiac sarcoplasmic reticulum. Effects of synthetic phospholamban peptides on Ca^{2+} pump ATPase. J. Biol. Chem. **267**, 1674–1679

50 Toyofuku, T., Kurzydlowski, K., Tada, M. and MacLennan, D. H. (1994) Amino acids Glu^2 to Ile^{18} in the cytoplasmic domain of phospholamban are essential for functional association with the Ca^{2+}-ATPase of sarcoplasmic reticulum. J. Biol. Chem. **269**, 3088–3094

51 Cantilina, T., Sagara, Y., Inesi, G. and Jones, L. R. (1993) Comparative studies of cardiac and skeletal sarcoplasmic reticulum ATPases. Effect of a phospholamban antibody on enzyme activation by Ca^{2+}. J. Biol. Chem. **268**, 17018–17025

52 Kimura, Y., Inui, M., Kadoma, M., Kijima, Y., Sasaki, T. and Tada, M. (1991) Effects of monoclonal antibody against phospholamban on Ca^{2+} pump ATPase of cardiac sarcoplasmic reticulum. J. Mol. Cell. Cardiol. **23**, 1223–1230

53 Cornea, R. L., Autry, J. M., Chen, Z. and Jones, L. R. (2000) Evidence for a direct functional interaction between leucine zipper residues of phospholamban and the Ca-pump of cardiac sarcoplasmic reticulum. Biophys. J. **76**, 75a

54 Asahi, M., McKenna, E., Kurzydlowski, K., Tada, M. and MacLennan, D. H. (2000) Physical interactions between phospholamban and sarco(endo)plasmic reticulum Ca^{2+}-ATPase are dissociated by elevated Ca^{2+}, but not by phospholamban phosphorylation, vanadate, or thapsigargin and are enhanced by ATP. J. Biol. Chem. **275**, 15034–15038

55 Xu, Z. C. and Kirchberger, M. A. (1989) Modulation by polyelectrolytes of canine cardiac microsomal Ca^{2+} uptake and the possible relationship to phospholamban. J. Biol. Chem. **264**, 16644–16651
56 Asahi, M., Kimura, Y., Kurzydlowski, K., Tada, M. and MacLennan, D. H. (1999) Transmembrane helix M6 in sarco(endo)plasmic reticulum Ca^{2+}-ATPase forms a functional interaction site with phospholamban. J. Biol. Chem. **274**, 32855–32862
57 Kimura, Y., Kurzydlowski, K., Tada, M. and MacLennan, D. H. (1996) Phospholamban regulates the Ca^{2+}-ATPase through intramembrane interactions. J. Biol. Chem. **271**, 21726–21731
58 Arkin, I. T., Adams, P. D., Brünger, A. T., Smith, S. O. and Engelman, D. M. (1997) Structural perspectives of phospholamban, a helical transmembrane pentamer. Annu. Rev. Biophys. Biomol. Struct. **26**, 157–179
59 Kimura, Y., Kurzydlowski, K., Tada, M. and MacLennan, D. H. (1997) Phospholamban inhibitory function is activated by depolymerization. J. Biol. Chem. **272**, 15061–15064
60 Chen, L., Yao, Q., Brungardt, K., Squier, T. and Bigelow, D. (1998) Changes in spatial arrangement between individual Ca-ATPase polypeptide chains in response to phospholamban phoshorylation. Ann. N.Y. Acad. Sci. **853**, 264–266
61 Autry, J. M. and Jones, L. R. (1997) Functional co-expression of the canine cardiac Ca^{2+} pump and phospholamban in *Spodoptera frugiperda* (Sf21) cells reveals new insights on ATPase regulation. J. Biol. Chem. **272**, 15872–15880
62 Cornea, R. L., Jones, L. R., Autry, J. M. and Thomas, D. D. (1997) Mutation and phosphorylation change the oligomeric structure of phospholamban in lipid bilayers. Biochemistry **36**, 2960–2967
63 Reddy, L. G., Jones, L. R. and Thomas, D. D. (1999) Depolymerization of phospholamban in the presence of Ca^{2+} pump: a fluorescence energy transfer study. Biochemistry **38**, 3954–3962

Received 8 December 1999/3 July 2000; accepted 24 July 2000

64 Li, M., Cornea, R. L., Autry, J. M., Jones, L. R. and Thomas, D. D. (1998) Phosphorylation-induced structural changes in phospholamban and its mutants, detected by intrinsic fluorescence. Biochemistry **37**, 7869–7877
65 Huggins, J. P. and England, P. J. (1987) Evidence for a phosphorylation-induced conformational change in phospholamban from the effects of three proteases. FEBS Lett. **217**, 32–36
66 Mortishire-Smith, R. J., Pitzenberger, S. M., Burke, C. J., Middaugh, C. R., Garsky, V. M. and Johnson, R. G. (1995) Solution structure of the cytoplasmic domain of phospholamban: phosphorylation leads to a local perturbation in secondary structure. Biochemistry **34**, 7603–7613
67 Maslennikov, I. V., Sobol, A. G., Anagli, J., James, P., Vorherr, T., Arseniev, A. S. and Carafoli, E. (1995) The secondary structure of phospholamban: a two dimensional NMR study. Biochem. Biophys. Res. Commun. **217**, 1200–1207
68 Kinosita, K., Ishiwata, S., Yoshimura, H., Asai, H. and Ikegami, A. (1984) Submicrosecond and microsecond rotational motions of myosin head in solution as revealed by time-resolved optical anisotropy measurements. Biochemistry **23**, 5963–5975.
69 Anderson, R. L. (1987) Practical Statistics for Analytical Chemists, Van Nostrand Reinhold, New York
70 Toyoshima, C., Sasabe, H. and Stokes, D. L. (1993) Three-dimensional cryo-electron microscopy of the Ca^{2+} ion pump in the sarcoplasmic reticulum membrane. Nature (London) **362**, 469–471
71 Ogawa, H., Stokes, D. L., Sasabe, H. and Toyoshima, C. (1998) Structure of the Ca^{2+} pump of sarcoplasmic reticulum: a view along the lipid bilayer at 9-Å resolution. Biophys. J. **75**, 41–52
72 Toyoshima, C., Nakasako, M., Nomura, H. and Ogawa, H. (2000) Crystal structure of the Ca^{2+} pump of sarcoplasmic reticulum at 2.6 Å resolution. Nature (London) **405**, 647–655